REGULAR ARTICLE

blood neoplasia

Dose escalation study of the HLA-A2-WT1 CD3 bispecific antibody RO7283420 in relapsed/refractory acute myeloid leukemia

Martin Hutchings,[1,2,*] Koorosh Korfi,[3,*] Pau Montesinos,[4] Armando Santoro,[5,6] Hsin-An Hou,[7] Pilar Martinez-Sanchez,[8] Susana Vives,[9] Sara Galimberti,[10] Tsai-Yun Chen,[11] Marco Frigeni,[12] Sylvain Garciaz,[13] Olga Salamero Garcia,[14] Su-Peng Yeh,[15] Karen Yee,[16] Jordi Esteve,[17] Ashish Bajel,[18] Shaun Fleming,[19] Anne Catherine Bretz,[20] Jan Attig,[21] Min Sun,[21] Sina Nassiri,[22] Tobias Rutishauser,[21] Christian Klein,[3] Y. May Ma,[22] Gabriel Schnetzler,[22] Stephanie Vauleon,[21] Huixin Yu,[21] Teresa Barata,[23] Muriel Richard,[3] Silke Simon,[21] Heather Hinton,[24] Nino Keshelava,[3] and Marion Subklewe[25]

[1]Department of Hematology and Phase 1 Unit, Rigshospitalet, and [2]Department of Clinical Medicine, University of Copenhagen, Copenhagen, Denmark; [3]Roche Pharma Research and Early Development, Oncology, Roche Innovation Center Zurich, Schlieren, Switzerland; [4]Department of Hematology, University Hospital of La Fe in Valencia, Valencia, Spain; [5]Department of Biomedical Sciences, Humanitas University, Milan, Italy; [6]Medical Oncology and Hematology Unit, Istituto di Ricovero e Cura a Carattere Scientifico Humanitas Research Hospital - Humanitas Cancer Center, Milan, Italy; [7]Division of Hematology, Department of Internal Medicine, National Taiwan University Hospital, Taipei, Taiwan; [8]Department of Hematology, Hospital Universitario 12 de Octubre, Madrid, Spain; [9]Departament de Medicina, Hospital Universitario Germans Trias i Pujol-Institut Català d'Oncologia Badalona, Josep Carreras Research Institute, Universitat Autònoma de Barcelona, Badalona, Spain; [10]Department of Clinical and Experimental Medicine, Section of Hematology, University of Pisa, Pisa, Italy; [11]Division of Hematology-Oncology, National Cheng Kung University Hospital, Tainan, Taiwan; [12]Department of Oncology and Hematology, Azienda Sociosanitaria Territoriale Papa Giovanni XXIII, Bergamo, Italy; [13]Department of Hematology, Aix-Marseille University, INSERM, Centre national de la recherche scientifique, Institut Paoli-Calmettes, Centre de Recherche en Cancérologie de Marseille, Marseille, France; [14]Department of Hematology, Hospital Universitari Vall d'Hebron, Vall d'Hebron Institute of Oncology, Barcelona, Spain; [15]Department of Internal Medicine, China Medical University Hospital, Taichung, Taiwan; [16]Cancer Clinical Research Unit, Princess Margaret Cancer Centre, Toronto, ON, Canada; [17]Department of Hematology, Hospital Clinic de Barcelona, Barcelona, Spain; [18]Department of Clinical Haematology, Peter MacCallum Cancer Centre and The Royal Melbourne Hospital, Melbourne, VIC, Australia; [19]Department of Hematology, The Alfred Hospital and Australian Centre for Blood Diseases, Monash University, Melbourne, Australia; [20]Roche Pharma Research and Early Development, Oncology, Roche Innovation Center Munich, Penzberg, Germany; [21]Roche Pharma Research and Early Development, Pharmaceutical Sciences, [22]Roche Pharma Research and Early Development, Oncology, and [23]Roche Product Development, Data Science, Roche Innovation Center, Basel, Switzerland; [24]Product Development Safety, F. Hoffmann-La Roche Ltd, Basel, Switzerland; and [25]Department of Medicine III, University Hospital, Ludwig Maximilian University Munich, Munich, Germany

Key Points

- RO7283420, a TCB engaging CD3 and Wilms tumor protein 1, demonstrated pharmacodynamic activity in this phase 1 study.
- RO7283420 was discontinued because of the lack of an exposure-response relationship and limited clinical efficacy.

A novel T-cell bispecific antibody (TCB), RO7283420, engaging CD3 and the HLA-A2-Wilms tumor protein 1 complex, was evaluated in this phase 1 study to characterize safety and tolerability, determine the maximum tolerated dose (MTD), and recommend a phase 2 dose for patients with relapsed/refractory acute myeloid leukemia in 2 groups: hematologic (group I, n = 57) and molecular (group 2, n = 5) relapse. In group I, 51 received RO7283420 intravenously (IV) and 6 subcutaneously. The IV doses ranged from 0.15-4 mg (flat; n = 13), 3-18 mg (step-up; n = 34) every 3 weeks, or 9 mg weekly (step-up; n = 4). The MTD was 1/3/12 mg every 3 weeks. The most frequent adverse event in the overall population was cytokine release syndrome (61.3%) with grade ≥3 recorded in 9.7% of patients. Twelve dose-limiting toxicities were reported in 11 patients and 12 (19.4%) grade 5 adverse events, including 1 hemophagocytic lymphohistiocytosis case related to RO7283420. Among the 42 efficacy-evaluable IV patients in group I, 4.8% achieved complete remission (CR), and 2.4% achieved CR with incomplete hematologic recovery. RO7283420 induced pharmacodynamic changes in peripheral blood (PB) at doses ≥1 mg, including significant T-cell activation and expansion in the PB and bone marrow (BM). Significant associations were found between

Submitted 16 December 2024; accepted 30 March 2025; prepublished online 11 May 2025. https://doi.org/10.1016/j.bneo.2025.100110.

*M.H. and K.K. are joint first authors.

Qualified researchers may request access to individual patient-level data through the clinical study data request platform (https://vivli.org/). Further details on Roche's criteria for eligible studies are available at https://vivli.org/members/ourmembers/. For further details on Roche's Global Policy on the Sharing of Clinical Information and how to request access to related clinical study documents, follow https://www.roche.com/research_and_development/who_we_are_how_we_work/clinical_trials/our_commitment_to_data_sharing.htm.

The full-text version of this article contains a data supplement.

© 2025 American Society of Hematology. Published by Elsevier Inc. Licensed under Creative Commons Attribution-NonCommercial-NoDerivatives 4.0 International (CC BY-NC-ND 4.0), permitting only noncommercial, nonderivative use with attribution. All other rights reserved.

blast reduction and baseline immunophenotype, including lower regulatory T cells and higher non-exhausted $CD8^+$ T cells in BM. Although dose escalation was discontinued because of limited efficacy and lack of an exposure-BM response relationship, the observed pharmacodynamics underscore the promising potential of this class of TCBs targeting intracellular antigens. This trial was registered at www.clinicaltrials.gov as #NCT04580121.

Introduction

Acute myeloid leukemia (AML) is a heterogeneous and aggressive hematologic malignancy.[1,2] Despite considerable progress in the development of novel therapies,[2] the prognosis for relapsed/refractory (R/R) AML remains poor.[3] Patients with R/R AML or molecular R/R AML with persistent measurable residual disease (MRD) after induction chemotherapy present an important unmet medical need.[4]

Wilms tumor protein 1 (WT1), an intracellular oncogenic protein, has been identified as a potential target for immunotherapy in AML.[5] Targeting intracellular antigens may increase the specificity and alleviate on-target, off-tumor toxicity in contrast with targeting myeloid lineage antigens.[6,7] WT1 is overexpressed in certain solid tumors and hematologic malignancies, including AML,[8] and has been suggested to be a predictive marker after chemotherapy[9,10] or allogeneic transplantation.[11]

In adults, WT1 expression is restricted to a small percentage of cells in very few tissues.[12] Adoptive cell therapy with T-cell receptor (TCR) transgenic T cells that target WT1 was shown to prolong relapse-free survival after hematopoietic stem cell transplantation (HSCT) in patients with high-risk AML.[13] In addition, vaccination with dendritic cells electroporated with WT1 messenger RNA was shown to reduce the risk for relapse after standard chemotherapy[14] and induce antigen-specific immune responses in patients with AML in complete remission (CR).[15]

RO7283420 (RG6007) is an off-the-shelf, novel, TCR-like T-cell bispecific antibody (TCB) with a 2:1 head-to-tail molecular format.[6] It engages CD3ϵ (monovalent binding) and the RMFPNAPYL peptide of the WT1 protein (bivalent binding), which is presented by the major histocompatibility complex-I HLA-A*02 after intracellular breakdown of WT1.[6] Simultaneous binding of both targets leads to T-cell activation and apoptosis of cells that express and present WT1.[6] Preclinical evaluation of RO7283420 in in vivo humanized AML xenografts and ex vivo AML blast co-culture

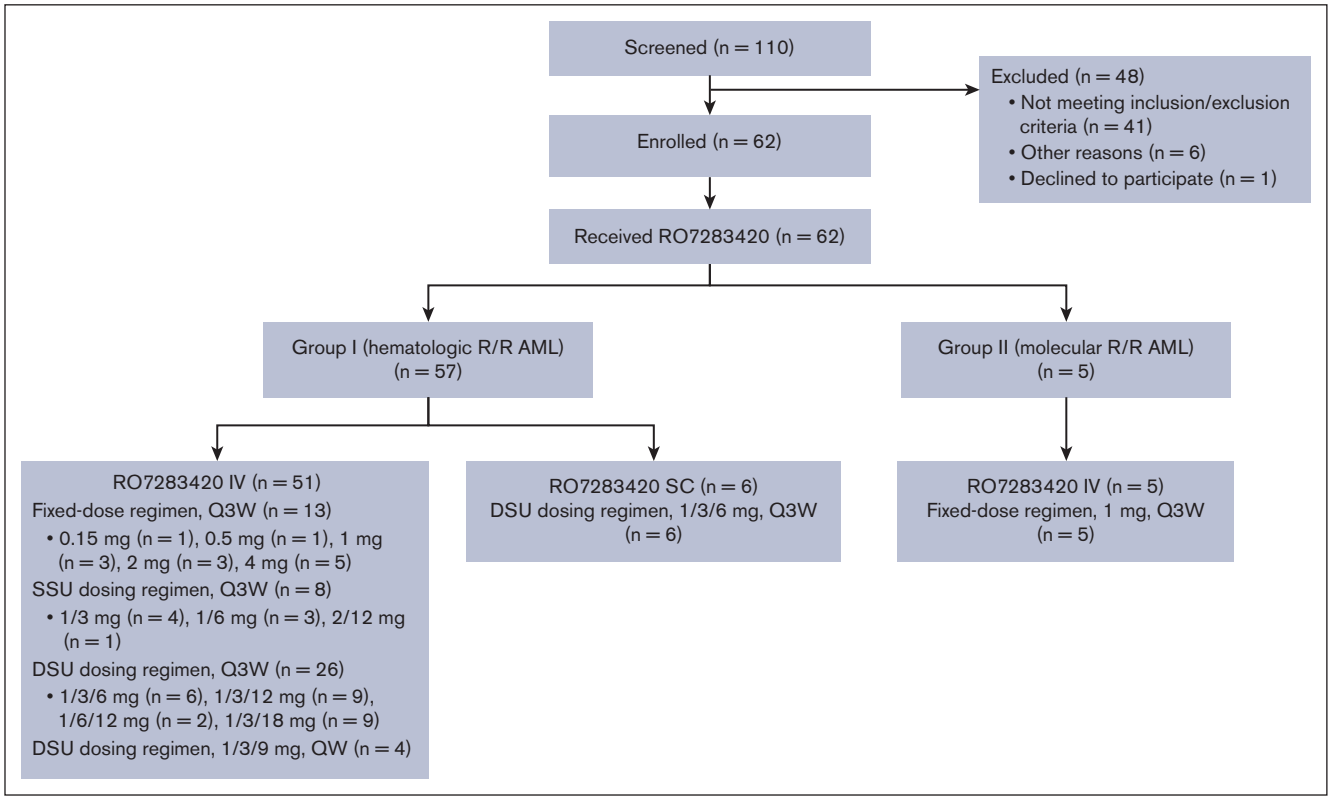

Figure 1. Patient consort flow diagram. AML, acute myeloid leukemia; DSU, double step-up; IV, intravenous; Q3W, every 3 weeks; QW, every week; R/R, relapsed or refractory; SC, subcutaneous; SSU, single step-up.

Table 1. Demographics, baseline disease characteristics, and previous therapies for the overall population and group I patients who received RO7283420 IV

	Overall population (N = 62)	Group I, IV administration (n = 51)
Age, median (range), y	65.5 (35-84)	66 (35-84)
≥65 years, n (%)	36 (58.1)	30 (58.8)
Male sex, n (%)	34 (54.8)	30 (58.8)
Race, n (%)		
Asian	10 (16.1)	8 (15.7)
White	50 (80.6)	41 (80.4)
Unknown	2 (3.2)	2 (3.9)
ECOG PS, n (%)		
0	36 (58.1)	29 (56.9)
1	23 (37.1)	19 (37.3)
2	3 (4.8)	3 (5.9)
Primary refractory, n (%)	23 (37.1)	21 (41.2)
Relapsed, n (%)	34 (54.8)	30 (58.8)
ELN risk category, n (%)		
Favorable	6 (9.7)	5 (9.8)
Intermediate	22 (35.5)	19 (37.3)
Adverse	32 (51.6)	25 (49)
Missing	2 (3.2)	2 (3.9)
BM blast count category, n (%)		
<30%	28 (45.2)	20 (39.2)
≥30 to <50%	13 (21)	13 (25.5)
≥50%	19 (30.6)	17 (33.3)
Missing	2 (3.2)	1 (2)
Number of previous AML therapies		
Median (range)	2 (1-5)	2 (1-5)
1, n (%)	14 (22.6)	7 (13.7)
2, n (%)	28 (45.2)	25 (49)
>2, n (%)	20 (32.3)	19 (37.3)
Previous HSCT, n (%)	18 (29)	15 (29.4)
Previous AML therapy, induction/re-induction, n (%)*	58 (93.5)	48 (94.1)
Cytarabine	48 (77.4)	39 (76.5)
Idarubicin	29 (46.8)	24 (47.1)
Fludarabine	22 (35.5)	18 (35.3)
Azacitidine	18 (29.0)	15 (29.4)
Daunorubicin	17 (27.4)	15 (29.4)
Venetoclax	16 (25.8)	15 (29.4)
Gemtuzumab	6 (9.7)	6 (11.8)
Previous AML therapy, consolidation/conditioning/maintenance/ other, n (%)*	40 (64.5)	34 (66.7)
Cytarabine	25 (40.3)	21 (41.2)
Azacitidine	22 (35.5)	18 (35.3)
Venetoclax	13 (21.0)	12 (23.5)
Fludarabine	10 (16.1)	8 (15.7)

AML, acute myeloid leukemia; BM, bone marrow; ECOG, Eastern Cooperative Oncology Group; ELN, European LeukemiaNet; HSCT, hematopoietic stem cell transplantation; IV, intravenous; PS, performance status.

*Data are displayed for the therapies that were received by ≥10% of patients in group I who received IV RO7283420.

Table 2. Genetic mutations detected in the overall population and in group I patients who received RO7283420 IV*

Mutation detected, n (%)	Overall population (N = 59)	Group I, IV administration (n = 49)
RUNX1	12 (20.3)	11 (22.4)
ASXL1	10 (16.9)	8 (16.3)
TP53	7 (11.9)	6 (12.2)
FLT3-ITD	5 (8.5)	3 (6.1)
NPM1	4 (6.8)	3 (6.1)
CEBPA	0	0
FLT3-TKD	0	0

*Percentages are calculated based on the total number of patients tested for the respective gene mutation. IV, intravenous.

models showed potent T-cell–mediated killing of primary AML cells.[6]

In this article, we present the results of a first-in-human study that evaluated the safety, tolerability, efficacy, pharmacokinetics (PK), and pharmacodynamics of RO7283420 in patients with R/R AML.

Methods

Study design and patient eligibility

This open-label, multicenter, phase 1, dose escalation and expansion study (NCT04580121) investigated single-agent RO7283420 in patients with hematologic or molecular R/R AML. Hematologic R/R AML was defined as failure to achieve CR or CR with incomplete hematologic recovery (CRi) after 2 induction attempts or first relapse after an unsuccessful salvage attempt, or second or later relapse, according to the 2017 European LeukemiaNet (ELN) recommendations.[16] Molecular R/R AML was defined as patients in CR (or CRi) with positive MRD according to local multiparameter flow cytometry or molecular assessment in compliance with the ELN consensus.[17] In this study, patients with hematological R/R AML were enrolled in group I and patients with molecular R/R AML were enrolled in group 2. All patients previously exhausted standard-of-care treatment with no other standard-of-care options available.

Eligible patients were aged ≥18 years with a confirmed diagnosis of primary or secondary AML according to the World Health Organization classification 2016 with measurable disease and confirmed genotype of HLA-A*02. Evidence of expression of WT1 protein was not required before study entry. All patients had an Eastern Cooperative Oncology Group performance status of 0 to 2, adequate renal and liver function, and peripheral blast counts ≤20 000/mm^3 on cycle 1 day 1 before the first dosing (supplemental Methods 1).

Patients were ineligible for the study if they had acute promyelocytic leukemia, core-binding factor AML (unless they received at least 2 salvage treatments), HSCT performed within 90 days of the first RO7283420 dose, clinical evidence or history of central nervous system leukemia, or presence of extramedullary disease (supplemental Methods 2).

The study was planned to consist of part A with single-patient dose escalation cohorts (group I), part B with multiple-patient dose escalation cohorts (groups I and II), and part C with dose expansion cohorts (groups I and II; supplemental Figure 1). The study was terminated before starting the dose expansion phase.

In part A, the starting dose of 0.15 mg was given as a fixed dose every 3 weeks through intravenous (IV) administration. The starting dose was selected based on an integrated pharmacokinetic/pharmacodynamic model that predicted the minimal anticipated

Table 3. Safety of RO7283420 in the overall population and by group and mode of administration

AE, n (%)	Overall population (N = 62)	Group I, IV administration (n = 51)	Group I, SC administration (n = 6)	Group II, IV administration (n = 5)
Any AE	61 (98.4)	50 (98)	6 (100)	5 (100)
Any treatment-related AE*	51 (82.3)	42 (82.4)	5 (83.3)	4 (80)
Grade 3 AE	46 (74.2)	41 (80.4)	3 (50)	2 (40)
Grade 3 treatment-related AE*	13 (21)	11 (21.6)	1 (16.7)	1 (20)
Grade 4 AE	10 (16.1)	6 (11.8)	3 (50)	1 (20)
Grade 4 treatment-related AE*	3 (4.8)	1 (2)	1 (16.7)	1 (20)
Deaths	49 (79)	44 (86.3)	4 (66.7)	1 (20)
Grade 5 AE	12 (19.4)	11 (21.6)	1 (16.7)	0
Grade 5 treatment-related AE*	1 (1.6)	1 (2)	0	0
Serious AE	48 (77.4)	42 (82.4)	4 (66.7)	2 (40)
Serious treatment-related AE*	25 (40.3)	21 (41.2)	3 (50)	1 (20)
Event that qualifies as DLT	11 (17.7)	8 (15.7)	2 (33.3)	1 (20)

*Considered by the investigator to be related to RO7283420. AE, adverse event; DLT, dose-limiting toxicity; IV, intravenous; SC, subcutaneous.

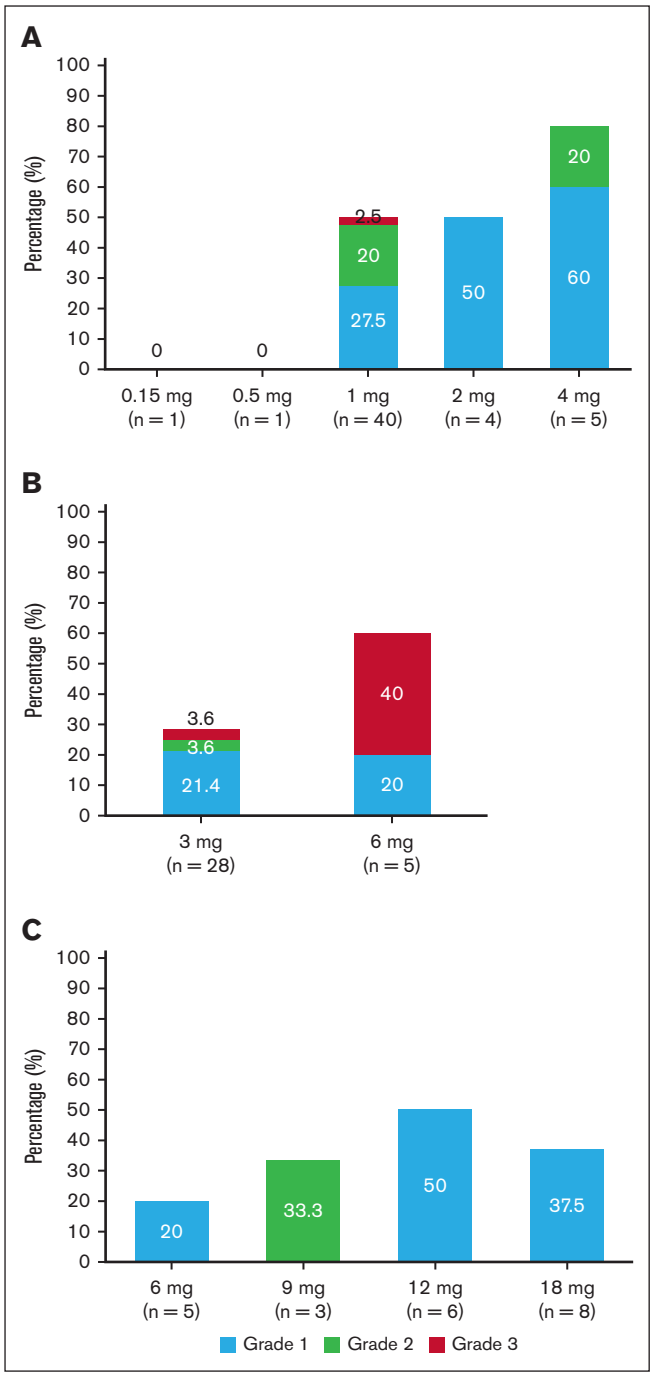

Figure 2. Incidence of maximum CRS grade by RO7283420 IV dose in group I patients. (A) At cycle 1 day 1. (B) At cycle 1 day 8 in patients who received previous 1 mg step-up dosing. (C) At cycle 1 day 15 in patients who received previous 1/3 mg DSU dosing. CRS, cytokine release syndrome; DSU, double step-up; IV, intravenous.

biologic effect level in humans. This model incorporated desired effects, such as AML blast killing, but no undesired effects, such as cytokine release syndrome (CRS) and cell killing in liver spheroids.[18] In part B, fixed doses from 1 mg to 4 mg IV every 3 weeks were tested, followed by single step-up (SSU) and then double step-up (DSU) regimens with doses of up to 18 mg (supplemental Figure 2A-B). Step-up dosing was introduced in cycle 1 because of its potential to mitigate CRS.[19,20] In addition, 1 cohort with DSU and weekly IV dosing was tested with a target dose of 9 mg (supplemental Figure 2C). Dose escalation was conducted by a modified data-augmented continual reassessment method with overdose control design, described by Liu et al[21] and Zhu et al.[22] Dose escalation in the step-up dosing regimens was guided using a 3+3 design. Subcutaneous (SC) administration with a DSU every 3 weeks dosing regimen was investigated in 1 cohort in group I in part B because of its potential to mitigate CRS[19] and to increase drug administration convenience for patients. Furthermore, in part B, 1 dose level at a fixed 1 mg every 3 weeks IV regimen was administered in group 2. Because of limited tolerability of the SC regimen and slow enrollment in group 2, no dose escalations were performed.

The protocol allowed up to 6 or 18 treatment cycles, and 3 or 9 additional cycles in patients who achieved at least partial remission, with the every 3 weeks or weekly dosing regimens, respectively.

All patients received the following premedications before RO7283420 administration: 20 mg IV dexamethasone (mandatory during cycle 1, then only in case of toxicity in previous cycle); 500 to 1000 mg oral or IV paracetamol or acetaminophen; and 25 to 50 mg oral or IV diphenhydramine or an alternative antihistamine at equivalent dose. Patients were hospitalized for 24 to 48 hours following administration of the step-up doses, first target dose, and if CRS occurred after the previous administration. If needed, tocilizumab was administered for the treatment of severe CRS and dasatinib, a lymphocyte-specific protein kinase inhibitor shown to potently and reversibly inhibit TCB-mediated T-cell activation,[23] was administered for the treatment of severe off-target toxicity that may be associated with TCBs like RO7283420 that target HLA-presented peptides.

Response was assessed on day 1 of cycles 2 (optional), 3, 6, and 9, and at the end-of-treatment visit for those who received RO7283420 every 3 weeks, and on day 1 of cycles 2 (optional), 5, 14, and 23 and at the end-of-treatment visit for those who received RO7283420 every week. Supplemental Methods 3-6 contain details on other analyses.

All enrolled patients provided written informed consent. The institutional review board/independent ethics committee of each study site approved the protocol. This study was conducted in accordance with the principles of the Declaration of Helsinki.

End points

Primary end points were the maximum tolerated dose and/or recommended phase 2 dose per schedule of RO7283420 and the nature, frequency, and severity of adverse events (AEs) and dose-limiting toxicities (DLTs).

Other end points included the maximum reduction from baseline in bone marrow (BM) blast count, response rates (defined by ELN 2017[16]; supplemental Table 2), duration of response, PK profiles and parameters of RO7283420, the incidence and titer of antidrug antibodies (ADAs) against RO7283420, and the relationship between pharmacodynamic biomarkers and response. All end points are presented in supplemental Table 1.

Table 4. Incidence and grade of CRS by dose and cycle among group I patients who received RO7283420 IV

n (%)	Cycle 1, day 1 1 mg (n = 40)	Cycle 1, day 8 3 mg* (n = 28)	Cycle 1, day 15 6-18 mg† (n = 22)	Cycle 2, day 1 6-18 mg† (n = 6)	Cycle 3 to EOT 6-18 mg† (n = 10)
All grades	20 (50)	8 (28.6)	8 (36.4)	2 (33.3)	5 (50)
Grade 1	11 (27.5)	6 (21.4)	7 (31.8)	2 (33.3)	4 (40)
Grade 2	8 (20)	1 (3.6)	1 (4.5)	0	0
Grade 3	1 (2.5)	1 (3.6)	0	0	1 (10)

CRS, cytokine release syndrome; EOT, end of treatment; IV, intravenous.
*Following 1 mg step-up on day 1 in cycle 1.
†Following 1/3 mg double step-up dosing in cycle 1.

Statistical analysis

The safety and efficacy end points were analyzed using descriptive statistics. Efficacy was assessed in all patients who received at least 1 dose of RO7283420 and who had at least 1 response assessment. Safety was assessed in all patients who received at least 1 dose of RO7283420. Per protocol, no formal statistical model or hypothesis testing was conducted. No formal sample size calculation was performed with the number of patients enrolled dependent on the course of dose escalation.

Results

Patients

A total of 62 patients were enrolled in 17 centers between November 2020 and February 2023 across 2 groups, namely patients with hematologic R/R AML (group I) who received IV or SC RO7283420 and patients with molecular R/R AML (group 2) who received IV RO7283420 (Figure 1). All enrolled patients received at least 1 dose of RO7283420, and the median treatment duration was 42 days (range, 1 to 190).

The baseline demographics, disease characteristics, and previous therapies for group I patients who received IV RO7283420 are presented in Table 1, and those were broadly similar to the overall population, including group I patients who received SC RO7283420 and group 2 patients (supplemental Table 3). Mutations were reported in *RUNX1* (22.4%), *ASXL1* (16.3%), *TP53* (12.2%), *FLT3-ITD* (6.1%), and *NPM1* (6.1%) for group I patients who received IV RO7283420 (Table 2; supplemental Table 4).

Table 5. Efficacy of IV RO7283420 among group I patients as defined by the ELN 2017 recommendations

Best overall response, n (%)	Efficacy-evaluable patients (n = 42)
Objective response (CRMRD, CR, CRi, PR)	3 (7.1)
CRMRD–	0
CR	2 (4.8)
CRi	1 (2.4)
PR	0
SD	20 (47.6)
PD	16 (38.1)
Missing/not evaluable	3 (7.1)

CR, complete remission; CRi, complete remission with incomplete hematologic recovery; CRMRD-, complete remission with absence of measurable residual disease; ELN, European LeukemiaNet; IV, intravenous; PD, progressive disease; PR, partial remission; SD, stable disease.

Safety and tolerability

In the overall population, treatment-related AEs (TRAEs), grade 3 TRAEs, grade 4 TRAEs, and serious TRAEs occurred in 51 (82.3%), 13 (21.0%), 3 (4.8%), and 25 (40.3%) patients, respectively (Table 3). In total, 49 patients (79.0%) died during the study; the main cause of death was progressive disease or disease relapse (53.0%; n = 26). Twelve patients (19.4%) experienced a total of 13 grade 5 AEs, including pneumonia (n = 3), hemophagocytic lymphohistiocytosis (HLH; n = 2), sepsis (n = 2), and 1 case each of cerebrovascular accident, death, febrile bone marrow aplasia, febrile neutropenia, respiratory failure, and subarachnoid hemorrhage (supplemental Table 5). The grade 5 events were considered unrelated to RO7283420, except 1 of the 2 HLH events, which occurred in a group I patient 9 days after the last IV RO7283420 administration in cycle 4 day 1 (1/3/9 mg weekly) when the patient experienced grade 3 CRS and grade 1 immune effector cell-associated neurotoxicity syndrome. The other grade 5 HLH event was considered unrelated to RO7283420 and occurred in a group I patient 22 days after the last IV RO7283420 administration in cycle 3 day 1 (1/3/18 mg every 3 weeks).

A total of 12 DLTs were reported in 11 patients. Of those, 8 occurred in group I patients who received IV RO7283420, including 5 cases of grade 3 CRS (at 1/3, 2/12, 1/6/12, 1/3/18 mg doses) and 1 case each of grade 3 stomatitis (1/3/12 mg), grade 3 muscle weakness (1/3/18 mg), and grade 4 thrombocytopenia (1/3/18 mg). Grade 3 muscle weakness was experienced after the first target dose of 18 mg but did not lead to cumulative damage, nor a repeat after re-dosing, suggesting an immune-related toxicity, such as CRS or immune effector cell-associated neurotoxicity syndrome. The maximum tolerated dose was reached at 1/3/12 mg every 3 weeks for group I patients who received IV RO7283420. Two cases of grade 2 injection site reactions, leading to a delay of >14 days, occurred in group I patients who received SC RO7283420. One patient in group 2 experienced grade 4 decreased neutrophil and platelet counts (supplemental Table 6).

The most common (≥20%) treatment emergent AEs were CRS in 38 (61.3%) patients, febrile neutropenia in 15 (24.2%), pneumonia in 15 (24.2%), and pyrexia in 14 (22.6%; supplemental Table 7).

The incidence and grade of CRS for all dosing regimens are presented in supplemental Table 8. The median time from administration to CRS onset was 2.1 hours (range, 1.4 hours before end of infusion to 41.6 hours after infusion). Of the 38 patients who experienced CRS, 13 (34.2%) were treated with tocilizumab, 29 (76.3%) with corticosteroids, and 4 (10.5%) with a vasopressor. Three (7.9%) patients were admitted to the intensive care unit. The median duration of CRS was 2 days (range, 1 to 16 days). To

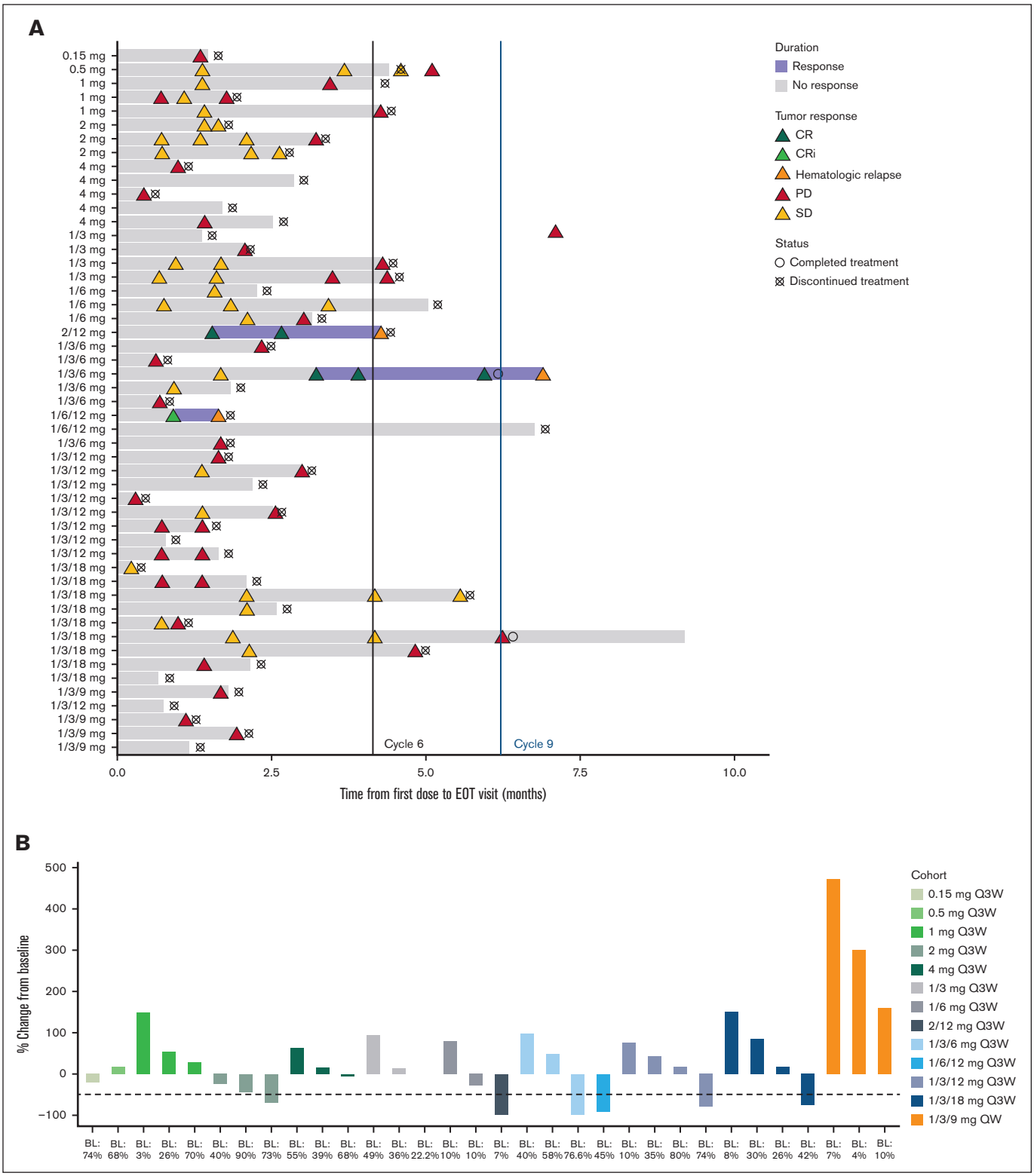

Figure 3. Duration of response and maximum blast count reduction in group I patients who received IV RO7283420. (A) Treatment follow-up and duration of response. (B) Maximum reduction from baseline in blast count in bone marrow. CR, complete remission; BL, baseline; CRi, complete remission with incomplete hematologic recovery; EOT, end of treatment; IV, intravenous; PD, progressive disease; SD, stable disease.

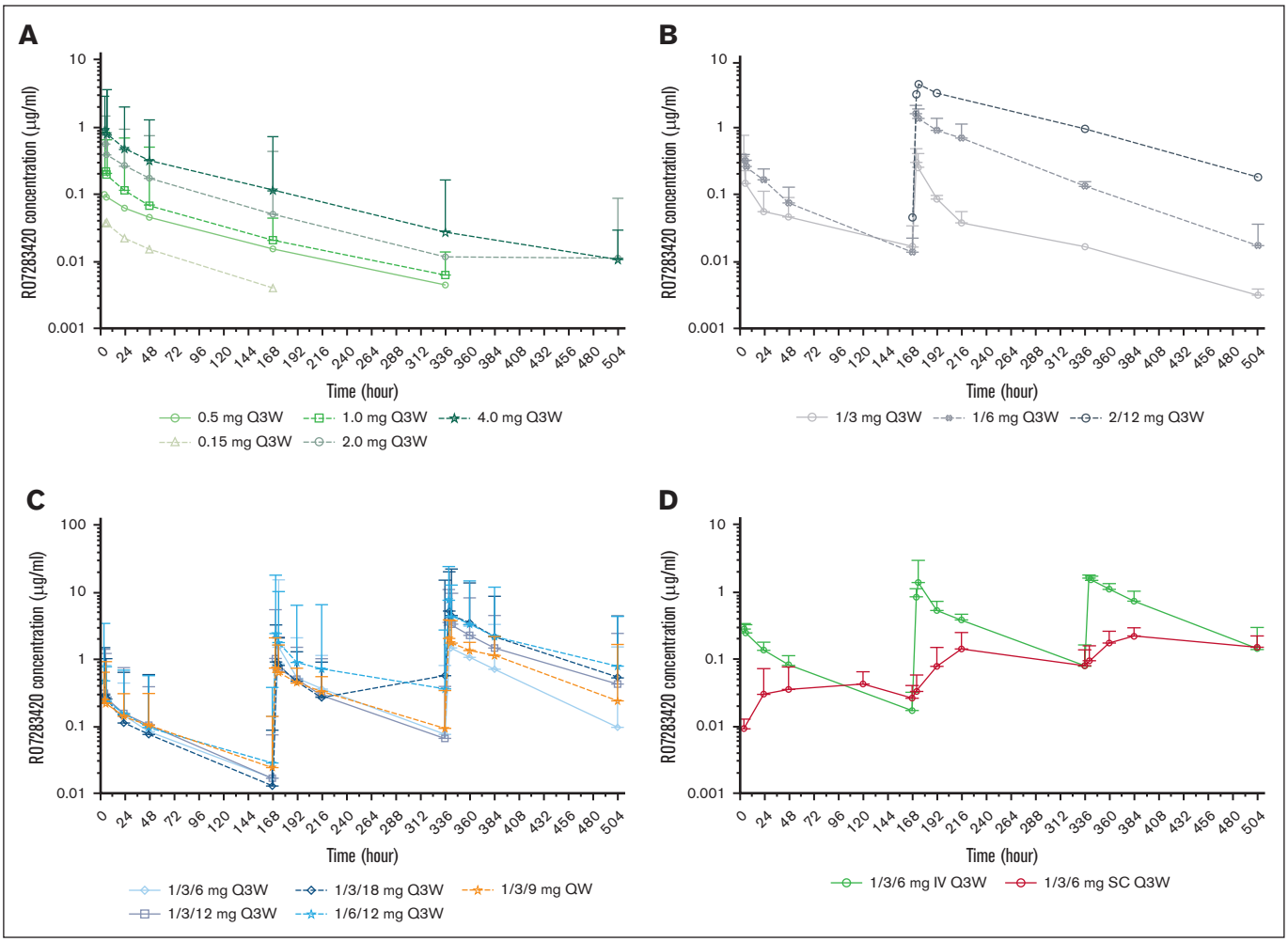

Figure 4. Pharmacokinetic profiles of RO7283420 in group I patients during cycle 1 following different dosing regimens. (A) Fixed IV dosing. (B) SSU dosing. (C) DSU IV dosing. (D) DSU SC dosing. DSU, double step-up; IV, intravenous; Q3W, every 3 weeks; QW, every week; SC, subcutaneous; SSU, single step-up.

manage the severity and incidence of CRS during the first doses of RO7283420, step-up dosing regimens were explored (supplemental Figure 2), including a DSU regimen of 1/3 mg given in cycle 1 day 1 and cycle 1 day 8, respectively, followed by a 6 to 18 mg target dose administered in cycle 1 day 15 and on day 1 of each cycle from cycle 2 onward. The 1 mg priming dose was shown to be sufficient to induce T-cell activation, as measured by the postinfusion increase in plasma cytokine levels (greater than or equal to twofold), and induced a more manageable CRS profile than an initial dose of 2 or 4 mg (supplemental Figures 2A and 3A). A dose of 3 mg was defined as the second step-up dose based on a safer CRS profile than 6 mg, and the target doses of 6 to 18 mg had similar CRS profiles (Figure 2B-C). Patients continued to experience sporadic CRS events in later cycles (Table 4).

The incidence and severity of reported CRS events after RO7283420 infusions were associated with elevated levels of inflammatory cytokines (eg, C-X-C motif chemokine ligand 10 [CXCL10], interferon gamma, interleukin-6, tumor necrosis factor) that were measured 2 and 24 hours after the end of infusions (supplemental Figure 3B). There was no clear relationship between the overall incidence or severity of CRS and the RO7283420 peak exposures (Cmax) after RO7283420 administration, except for cycle 1 day 8 for which a trend toward a higher CRS grade with higher Cmax was observed for patients treated with SSU and DSU regimens.

Efficacy

Because of the small sample sizes of group I patients who received SC RO7283420 and of group 2 and the limited availability of complete data sets, efficacy results are only reported for group I patients who received IV RO7283420.

Among the 42 efficacy-evaluable patients in group I who received IV RO7283420, 2 (4.8%) achieved CR at the dose levels of 2/12 mg and 1/3/6 mg and 1 (2.4%) achieved CRi at the dose level of 1/6/12 mg (Table 5). The duration of response for 2 patients who achieved CR was 35 days (censored observation, patient was discontinued from study because of an increase in MRD while the BM blast count was still below 5.0% and was switched to azacitidine) and 113 days (patient was discontinued from study because of an increasing blast count and received HSCT). The patient who achieved CRi was discontinued from the study by the physician's decision 24 days from response assessment (CRi) and was

Table 6. PK parameters of RO7283420 following a single IV dose in group I patients

	Dose (mg)				
Parameter	**0.15***	**0.5***	**1.0**	**2.0**	**4.0**
Tmax, n	1	1	39	3	5
Median, h*	5.93	4.08	4.17	4.37	4.17
Range, min-max, h	n/a	n/a	0.50-7	4.13-4.75	3.50-6.08
Cmax, n	1	1	39	3	5
Geo mean, µg/mL*	0.0388	0.100	0.274	0.560	0.944
Geo CV%, µg/mL	n/a	n/a	50.14	20.31	27.85
Cmax_D, n	1	1	39	3	5
Geo mean, ug/mL/mg*	0.259	0.200	0.287	0.28	0.244
Geo CV%, ug/mL/mg	n/a	n/a	45.58	20.31	24.56
AUC0-24, n	1	1	38	3	5
Geo mean, h*ug/mL*	0.681	1.78	3.98	7.75	14.2
Geo CV%, h*ug/mL	n/a	n/a	54.54	16.22	39.28
AUC0-168, n	1	1	26	3	5
Geo mean, h*ug/mL*	2.16	6.50	10.2	23.2	44.2
Geo CV%, h*ug/mL	n/a	n/a	62.74	53.55	51.1
DnormAUC168h, n	1	1	26	3	5
Geo mean, (h*ug/mL)/mg*	14.4	13.0	10.2	11.6	11.4
Geo CV%, (h*ug/mL)/mg	n/a	n/a	62.61	53.55	47.47
Terminal half-life, n	1	1	25	3	5
Median, h*	61.5	84.1	29.09	76.41	80.67
Range (min-max), h	n/a	n/a	7.46-74.6	26.5-119	34.2-90.2
Vss_obs, n	1	1	25	3	5
Geo mean, L*	4.99	6.79	3.81	5.72	6.27
Geo CV%, L	n/a	n/a	35	7.6	21
Cl_obs, n	1	1	25	3	5
Geo mean, mL/h*	59.0	58.1	90.7	69.4	72.9
Geo CV%, mL/h	n/a	n/a	63.79	80	59.87

AUC, area under the curve; Cl, clearance; DnormAUC168h, dose-normalized area under the curve from 0 h to 168 h post most recent dose; Geo CV, geometric coefficient of variation; Geo mean, geometric mean; h, hours; IV, intravenous; max, maximum; min, minimum; n/a, not applicable; obs, observed; PK, pharmacokinetic; Vss, volume of distribution at steady state.
*In case of n = 1 in a cohort, the individual values for the single participant are given.

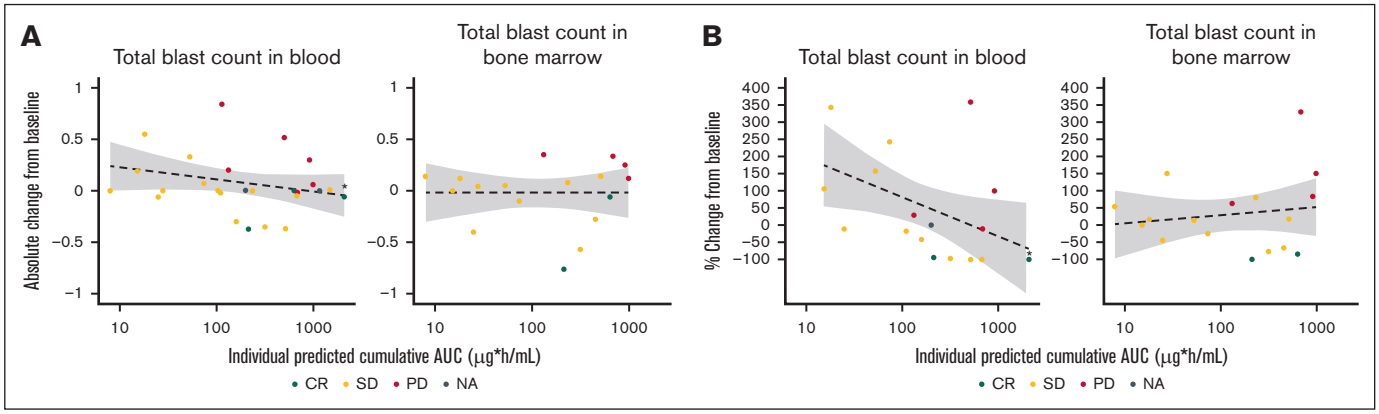

Figure 5. Exposure-response analysis for blast count reduction in PB and BM for group I patients who received IV RO7283420. (A) Total blast count reduction. (B) Percentage blast count reduction. The dashed line represents a linear regression of the data, and the shaded area shows the corresponding 95% confidence interval. The patient marked with an asterisk (*) has been retrospectively corrected from CR to NE. AUC, area under the curve; CR, complete remission; IV, intravenous; SD, stable disease; PD, progressive disease; NA, not available; NE, not evaluable.

Table 7. ADA status in the overall population

ADA status, n (%)	Overall population (N = 62)
Negative	49 (79)
Positive	13 (21)
Treatment induced*	12 (92.3)
Persistent	7 (58.3)
Transient	5 (41.7)
Treatment enhanced†	1 (7.7)

*Patients were considered treatment induced if they were ADA negative or missing data at baseline and developed an ADA response following study drug administration.

†Patients were considered treatment enhanced if they were ADA positive at baseline and the titer of one or more samples after baseline were greater than the titer of the baseline sample by a scientifically reasonable margin such as at least 4-fold. ADA, anti-drug antibody.

switched to mercaptopurine. Nine (21.4%) patients reached cycle 6 without disease progression, and 2 (4.8%) of them continued dosing up to cycle 9 (Figure 3A). No common demographic, disease characteristics, or previous treatments were identified among the responders.

Six (11.8%) patients achieved a best overall BM blast reduction of >50% from baseline; no dose-response relationship was observed (Figure 3B).

PK and exposure-response analysis

The cycle 1 PK profiles of patients who received IV RO7283420 in group I are displayed in Figure 4A-C.

Following IV infusion over 4 hours, the serum RO7283420 concentrations reached Cmax shortly after the end of infusion. The cycle 1 PK profiles of IV RO7283420 were overall dose-linear in the tested dose range of 0.15 to 18 mg with a biphasic disposition, composed of an initial rapid distribution phase, followed by a slower elimination phase. The median terminal elimination half-life after the first dose on cycle 1 day 1 ranged from 29 to 84 hours, whereas the clearance was highly variable (geometric means ranging from 69 to 91 mL/h) and independent of the administered dose or emergence of ADAs (Table 6).

After SC administration of RO7283420, serum exposures were measurable after 4 hours and peaked after 48 to 168 hours after the dose (Figure 4D). The peak concentrations were five- to eightfold lower than after IV administration of the same doses. The preliminary SC bioavailability was estimated to be ~76%.

A preliminary population PK model was developed for RO7283420 based on all IV PK data. The population and individual PK profiles were well described by a 2-compartment PK model with linear and saturable Michaelis-Menten elimination.

The relationship between RO7283420 serum exposure and blast response in peripheral blood (PB) and BM, defined as a reduction in blast count, was investigated for group I patients who received IV RO7283420. There was a trend toward an association between RO7283420 exposure (ie, cumulative area under the curve from day 1 to 42) and blast count reduction (both total and percentage) in the PB. No relationship between RO7283420 exposure and blast count reduction in the BM was observed (Figure 5).

Immunogenicity

Only a moderate incidence of ADA was observed with treatment-enhanced or treatment-induced (persistent or transient) ADAs in serum that occurred in 13 (21.0%) patients in the overall population (Table 7), and only 1 case coincided with reduced RO7283420 exposure. There was no association between any safety events and positive ADA titers.

Pharmacodynamics and molecular correlates of response

RO7283420 induced pharmacodynamic changes in PB at all tested doses ≥1 mg (supplemental Figure 3A). In line with the known mechanism of action (MoA)[24] and safety profile of TCBs,[25-28] an inflammatory cytokine release greater than or equal to twofold relative to baseline was observed 2 hours after the end of each infusion in cycle 1 with the largest increase observed after the first infusion (Figure 6A). The cytokine levels after infusion were associated with the reported incidence and severity of CRS events (supplemental Figure 3B) and was partially mitigated by step-up dosing (supplemental Figure 3A). The magnitude of soluble CD25 (IL2SR) and CXCL10 release, surrogates for T-cell activation, relative to baseline was associated with increasing exposure levels (cumulative area under the curve) at the end of cycle 1 (Figure 6B), indicating exposure-driven T-cell activation. Peripheral T-cell redistribution was observed after each dosing administration during cycle 1 (supplemental Figure 4) in line with the previously reported MoA of TCBs.[24] Furthermore, RO7283420 induced significant ($P < .05$) expansion of naïve, effector memory, and activated (4-1BB$^+$, CD28$^+$) CD8$^+$ and CD4$^+$ T cells in PB (Figure 6C-D) and activated (4-1BB$^+$, PD-1$^+$) and proliferating (Ki67$^+$) CD8$^+$ T cells in BM after 2 treatment cycles (Figure 6E-F); the latter is indicative of TCB-induced pharmacodynamic effects in the tumor microenvironment.

To further investigate the molecular correlates of response, the baseline PB and BM samples were evaluated to identify associations with the best blast reductions (≤−1 log odds ratio of best blast change measured from baseline [≥45% blast reduction]; supplemental Figure 5A, supplemental Methods 6) observed in each compartment respectively. The immunophenotype of baseline samples was analyzed using high-throughput spectral flow cytometry (BM and PB; supplemental Figures 6 and 7) and single-cell RNA sequencing (scRNA-seq; BM; supplemental Figure 8), followed by dimensionality reduction and clustering analysis. In BM, a significant ($P < .05$) association was identified with BM blast reduction and a lower frequency of CD4$^+$ T cells composed of regulatory T cells and central memory cells that co-expressed T-cell immunoreceptor with immunoglobulin and immunoreceptor tyrosine-based inhibition motif domain (TIGIT), CD95, and programmed cell death protein 1 (PD-1) (Cluster 4) and a higher frequency of nonexhausted (TIGIT$^-$) CD8$^+$ naïve T cells (CD45RA$^+$, CD197$^+$, CD57$^-$, CD95$^-$, Cluster 8; Figure 7A,C; supplemental Figure 6F-G). Similarly, scRNA-seq revealed a trend toward higher naïve-like CD8 and lower exhausted CD8 signature scores at baseline in the BM of patients who achieved a blast reduction (Figure 7D). In PB, a significant ($P < .05$) association was identified between PB blast reduction and a lower frequency of 3 clusters of CD8$^+$ T cells mainly composed of effector memory (CD45RA$^-$, CD197$^-$) and terminal effector memory T cells (TEMRA; CD45RA$^+$, CD197$^-$) that were potentially exhausted

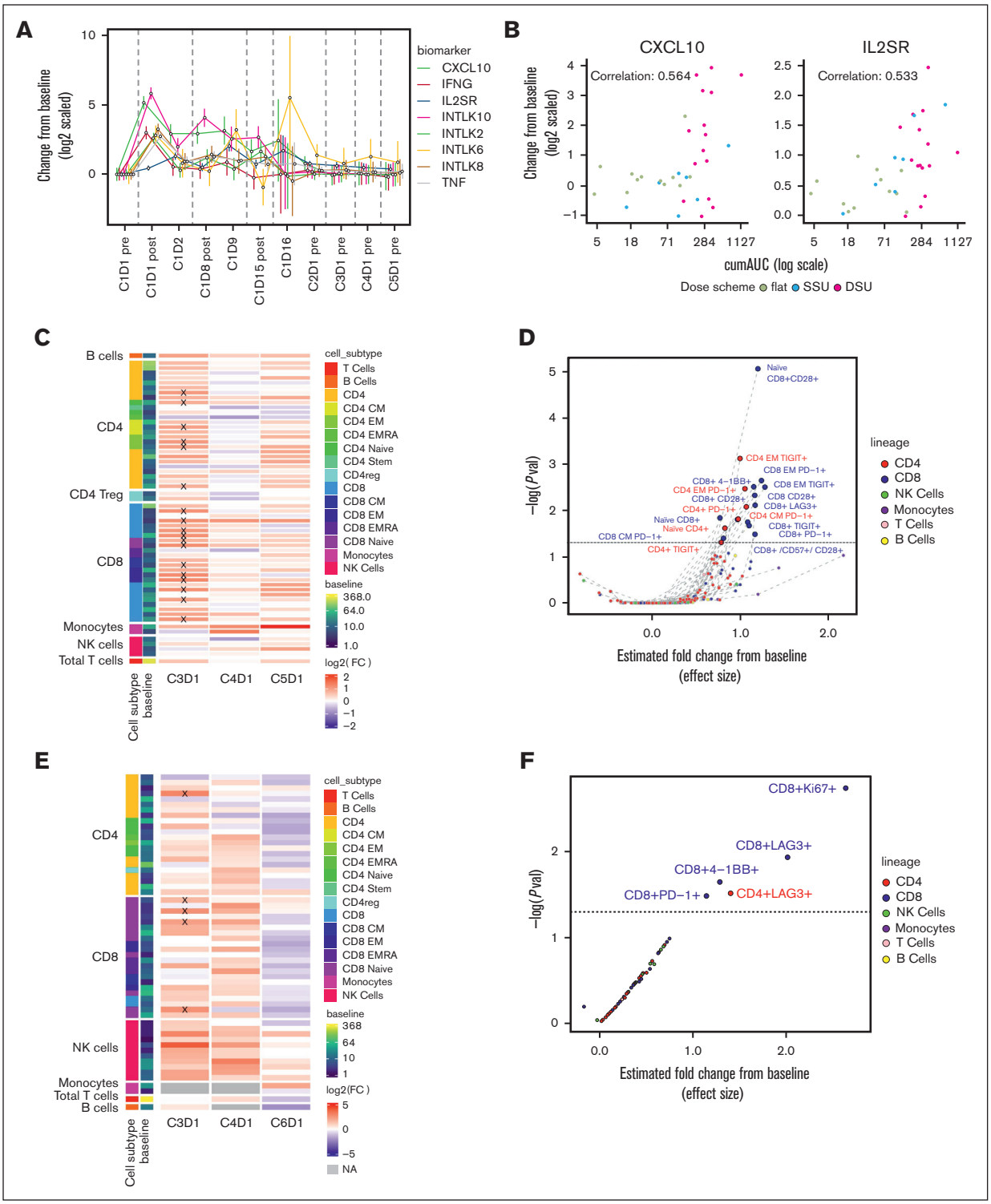

Figure 6. On-treatment pharmacodynamics in PB and BM aspirates support the expected MoA of a TCB. (A) Cytokine dynamics with estimated mean change from baseline across all patients with valid data at a given time point. The error bars indicate the 95% confidence interval, and dashed lines indicate RO7283420 administration. (B) Scatter plots showing the cumAUC vs log2-transformed change from baseline of soluble CD25 (IL2SR) and CXCL10 plasma levels at the end of cycle 1 (FDR-adjusted *P* value <.1; Brownian distance covariance test). Dose scheme group with flat, SSU, and DSU indicated. (C,E) Heatmap of immunophenotype on-treatment changes in PB (C) and BM aspirates (E) of absolute cell counts per µL shown as the log2-transformed fold change (log2[FC]) from baseline. Significantly changed immunophenotypes are labelled with an x (unadjusted *P* value <.05; linear mixed-effects model [C]; paired *t* test for C3D1 vs baseline comparison [E]). Baseline value (cells/µL) for each marker is indicated by the color gradient, and immune cell subtypes are indicated by the color coding. Grey cells indicate data that are not available. All time points are samples drawn before the dose administration of the indicated cycle. (D,F) Volcano plots of immunophenotype on-treatment vs baseline changes of absolute cell counts/µL in PB (D) and BM

(TIGIT$^+$) or primed for apoptosis (CD127$^-$) and/or highly differentiated and potentially senescent (CD57$^+$ and CD28; Figure 7B-C; supplemental Figure 7F-H). Overall, only 3 of 13 patients who achieved blast reductions in PB also saw similar reductions in BM, suggesting that the BM's less immunosuppressive microenvironment,[31,32] with more naïve T cells, may be key to a complete elimination of AML blasts.

Evaluating the reported molecular abnormalities in key AML driver genes (eg, *TP53*, *NPM1*, *FLT3*) or ELN risk categories at baseline revealed no association with the observed blast reductions (supplemental Figure 5B). The frequency of AML blasts in PB and BM measured by differential counts locally and by flow cytometry at a central laboratory were highly concordant (supplemental Figure 5C-D); however, the AML blast count at baseline was not significantly associated with the observed blast reductions (supplemental Figure 5E-F). In the absence of a direct measurement of WT1-peptide presented by HLA-A2, neither WT1 RNA levels in PB (Figure 7E) nor the frequency of WT1$^+$ or HLA-A2$^+$ blasts in PB or BM at baseline were associated with the observed blast reductions (Figure 7F). scRNA-seq analysis of AML cells (supplemental Figure 8A-B) in baseline and on-treatment BM samples revealed that WT1$^+$ AML cells were reduced in 8 of 10 patients on treatment, whereas the frequency of HLA-A$^+$ AML cells remained unchanged (Figure 7G). WT1$^+$ cells were differentially distributed in different AML cell subpopulations with leukemia stem and progenitor cells having the highest frequency of WT1$^+$ cells, whereas the monocyte-like subpopulation had the lowest abundance (Figure 7H). Upon disease progression, the monocyte-like cells expanded (>5%) in most patients (Figure 7I), and within the expanding monocyte-like subpopulation, the WT1$^+$ cells that co-expressed PSMB9 (a component of immunoproteasome machinery) were completely eliminated, whereas the WT1$^+$PSMB9$^-$ and WT1$^-$ cells remained (Figure 7J), indicating WT1$^-$ outgrowth and the expression of antigen-presenting machinery as potential escape mechanisms as previously reported.[33]

Discussion

There is a high unmet need for more effective treatment for R/R AML.[2-4,34] No bispecific antibody has been approved for AML, although numerous trials are underway to investigate, for example, CD33- or CD123-targeting TCBs.[35] TCBs that target intracellular antigens via HLA-peptide complexes offer a unique and novel approach by expanding therapeutic possibilities beyond cell surface markers. The intracellular antigen being targeted should have high tumor specificity, minimal expression in healthy tissues, and robust HLA presentation. Advanced tools to accurately measure HLA-antigen complex density are also required to select patients with high antigen expression and to ensure sufficient target engagement.

RO7283420 is the first TCR-like TCB that engages CD3ϵ and WT1 to be evaluated in AML.[6] WT1 was chosen as a target because of its high expression in AML cells, thereby minimizing off-target effects, and accessibility through presentation by HLA-A2.[6,36] Overall, the safety profile of RO7283420 was consistent with that of other TCBs in R/R AML, including CRS incidence.[25-27] Previous trials that investigated bispecific antibodies in R/R AML reported a high incidence of any grade CRS (50%-96%).[25-28] In this study, any grade CRS occurred in 38 (61.3%) patients, and grade 3 CRS, which occurred in 6 patients (9.7%), was the most common DLT, accounting for 5 of the 12 DLTs. Previous research has demonstrated that step-up dosing can reduce the incidence and severity of CRS[20]; most cases of severe CRS occur following the first dose of T-cell engaging therapy, and the time to onset is generally short after drug administration.[37] In this study, grade ≥3 CRS was observed following both the first and later infusions of RO7283420, and the use of step-up dosing reduced the incidence of CRS, particularly high-grade CRS. The time to onset of CRS events was generally soon after infusion.

HLH is a life-threatening clinical condition that is characterized by sustained immune system activation that leads to systemic severe hyperinflammation and multi-organ failure if left untreated.[38] HLH has been reported at a high incidence in patients with AML[39] and has been reported previously in patients treated with other T-cell engaging therapies.[40] Diagnosing HLH in patients with AML is particularly challenging because of overlapping symptoms and laboratory findings with the underlying AML disease.[41-43] Moreover, HLH has been reported in patients with AML, often in the context of infection[42,44] and disease progression.[41] In this study, 2 patients died after developing HLH, and 1 of these deaths was considered to be related to RO7283420.

The clearance of RO7283420 was relatively fast for an immunoglobulin G–based molecule with no relevant accumulation during weekly IV dosing. Despite pharmacodynamic evidence of T-cell activation and expansion in both PB and BM, as expected based on the MoA of TCBs, the overall clinical efficacy remained limited with CR/CRi rates of 7.1% in patients with hematologic R/R AML who were treated with IV RO7283420, albeit in line with the CR rates (0%-12%) reported in recent trials that investigated bispecific antibodies in R/R AML.[25-27,45] Although there was a trend toward an association between RO7283420 exposure and blast count reduction in PB, no relationship between RO7283420 exposure and blast count reduction in BM was observed at the explored dose ranges. Potential explanations for this discrepancy in the exposure-response observed in PB vs BM could be insufficient or variable exposure levels of RO7283420 in the BM and AML niche (ie, suggesting a need for higher doses) or the treatment schedule or reaching the target dose earlier (vs day 15) to control the fast-growing AML disease in which intense treatment in the first weeks of therapy may achieve a response.

Our analysis of baseline PB and BM samples indicated that a less immunosuppressive BM microenvironment and a more naïve and less exhausted CD8 T-cell phenotype were the key features

Figure 6 (continued) (F) shown as effect size vs $-\log_{10}$ transformed *P* values (−log[pval]). Effect size is the estimated mean fold change from baseline (D) and Cohen's D statistic at C3D1 vs baseline (F). Significantly expanded CD4$^+$ and CD8$^+$ T-cell populations are highlighted (unadjusted *P* value <.05 indicated by dashed horizontal line; linear mixed-effects model [D]; paired *t* test [F]). Cell subtypes are indicated by color coding. cumAUC, cumulative area under the curve; CxDx, Cycle x Day x; CM, central memory; CXCL10, C-X-C motif chemokine ligand 10; EM, effector memory; EMRA, terminally differentiated effector memory cells re-expressing CD45RA; FC, fold change; FDR, false discovery rate; IFNG, interferon gamma; INTLK, interleukin; MoA, mechanism of action; NK, natural killer; pre, pre-dose; post, post-dose 2 hours end of infusion; TCB, T-cell bispecific antibody; TNF, tumor necrosis factor; Treg, regulatory T cell.

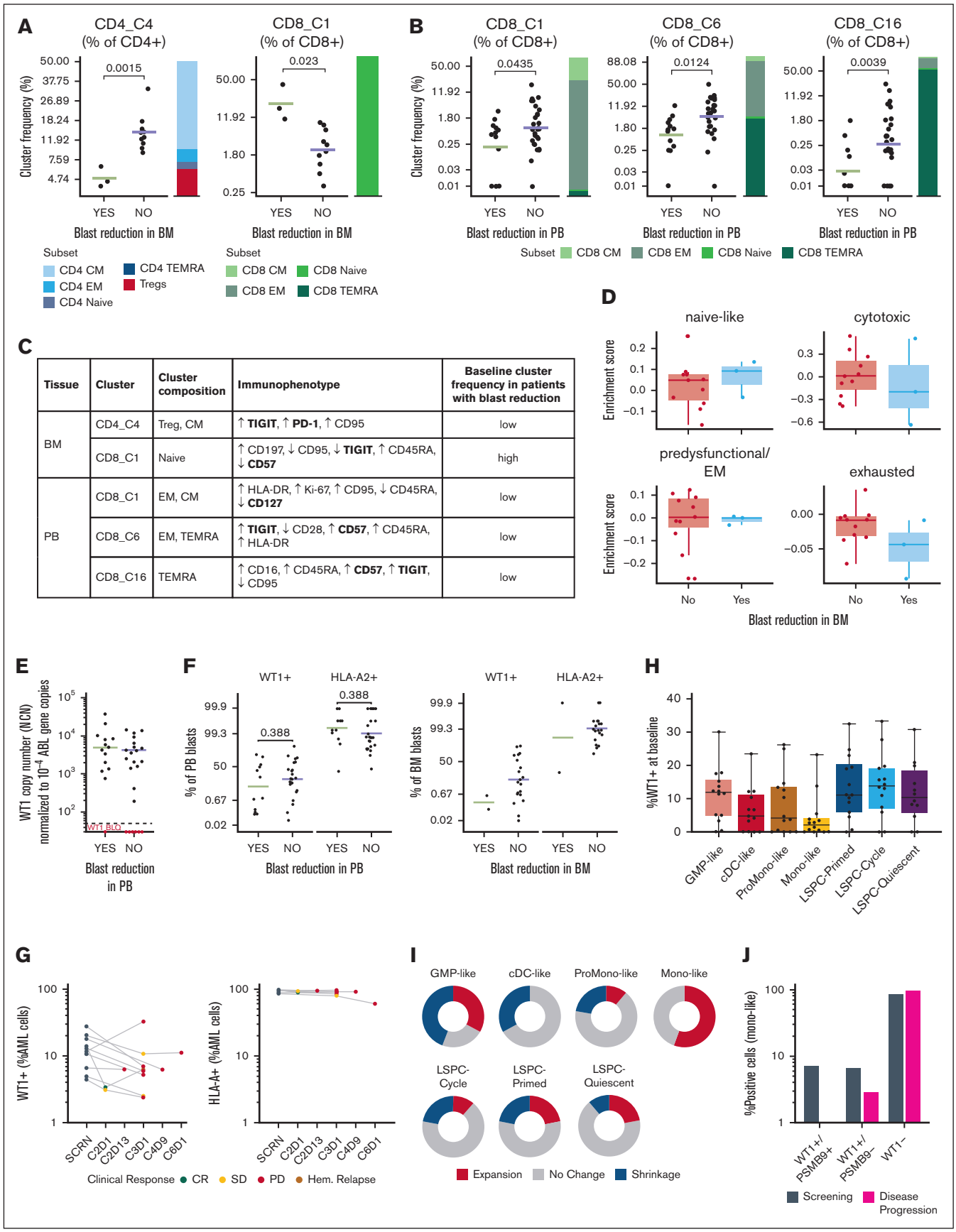

Tissue	Cluster	Cluster composition	Immunophenotype	Baseline cluster frequency in patients with blast reduction
BM	CD4_C4	Treg, CM	↑ **TIGIT**, ↑ **PD-1**, ↑ CD95	low
	CD8_C1	Naive	↑ CD197, ↓ CD95, ↓ **TIGIT**, ↑ CD45RA, ↓ **CD57**	high
PB	CD8_C1	EM, CM	↑ HLA-DR, ↑ Ki-67, ↑ CD95, ↓ CD45RA, ↓ **CD127**	low
	CD8_C6	EM, TEMRA	↑ **TIGIT**, ↓ CD28, ↑ **CD57**, ↑ CD45RA, ↑ HLA-DR	low
	CD8_C16	TEMRA	↑ CD16, ↑ CD45RA, ↑ **CD57**, ↑ **TIGIT**, ↓ CD95	low

Figure 7.

associated with blast reduction, highlighting the role of immune fitness in achieving response to TCBs as reported recently in R/R multiple myeloma[46] and diffuse large B-cell lymphoma.[47] T-cell exhaustion and senescence are prevalent in AML.[48] Enhancing T-cell function and eliminating immunosuppressive mechanisms with, for example, regulatory T cell depletors, T-cell costimulators, and checkpoint or histone deacetylase inhibitors,[48,49] should be considered to promote the efficacy of TCBs. TCBs may also be more effective in consolidative or maintenance settings, for example, following venetoclax/azacitidine treatment as shown in a recent study.[50]

The expression of WT1 in this study was heterogeneous with some AML cell subsets showing low to no WT1 expression, and measuring the abundance of WT1 peptide presented by HLA-A2 was also challenging. Furthermore, the immunoproteasome machinery plays a role in the escape mechanisms associated with immunotherapies that target intracellular antigens, such as WT1.[33] Therefore, targeting extracellular (eg, CD33, CD123, or CLL-1)[51,52] or intracellular (eg, preferentially expressed antigen in melanoma [PRAME] or mucin-1 [MUC1])[53,54] antigens with more constitutive and homogeneous expression on AML blasts and stem cells should be explored alone or in combination with WT1 peptide–targeted immunotherapies to ensure T-cell redirection to the AML niche and to minimize immune escape. In addition, combining TCBs that target intracellular antigens with therapies that enhance antigen processing and presentation (eg, epigenetic modulators, immunoproteasome activators, or interferons) may overcome poor or inconsistent antigen presentation by tumor cells.[55-57]

In conclusion, RO7283420 is the first TCR-like TCB that was evaluated in AML to our knowledge. We observed pharmacodynamic evidence of T-cell activation and expansion, however, at the explored doses, no clear drug exposure-response relationship and limited clinical efficacy were observed. The safety profile was shown to be consistent with other TCBs in R/R AML. Based on the totality of data, the study was discontinued.

Acknowledgments

The authors thank the patients for participating in the study. The authors give special thanks to the following subinvestigators for their contribution to the study: Serena Balducci, Veit Bücklein, Isabel Cano Ferri, Gladys Ibarra, Alba Puyuelo, Caroline Hasselbalch Riley, and Ana Triguero. The authors also give special thanks to Enrique Gomez Alcaide, Christina Godfried Sie, Rui Lopes, Brendan McAtarsney, and Joanne Hayward for their contributions to the biomarker analysis; to Olaf Broders for the development of the pharmacokinetics and antidrug antibody assays; to Paul Grimsey, Julie Janssen, and Christophe Boetsch for data analysis; to Yuying Xie for his contribution to the statistical analyses; to Nassim Sleiman, Jane Gao, and Daria Katalevska for statistical programming; to Tayo Bodede and Paula Reid for study conduct; and to Elisa Cinato for assistance in finalization of the manuscript.

Study WP42004 was sponsored by F. Hoffmann-La Roche Ltd. Medical writing assistance was provided by Mary Mullaney from nspm Ltd, Meggen, Switzerland, and funded by F. Hoffmann-La Roche Ltd.

Authorship

Contribution: K.K., A.C.B., J.A., M. Sun, S.N., T.R., C.K., Y.M.M., G.S., S. Vauleon, H.Y., T.B., M.R., S.S., H.H., and N.K. designed the trial; M.H., P.M., A.S., H.-A.H., P.M.-S., S. Vives, S. Galimberti, T.-Y.C., M.F., S. Garciaz, O.S.G., S.-P.Y., K.Y., J.E., A.B., S.F., and M. Subklewe enrolled patients; S.N. performed the single-cell RNA sequencing data analysis; S. Vauleon conducted the pharmacokinetics and antidrug antibody assay validations and sample

Figure 7. Baseline biomarkers associated with blast reduction in BM and PB. (A) BM blast reduction-associated immunophenotype clusters identified in BM after UMAP dimensionality reduction and FlowSOM clustering of high-dimensional cellular immunophenotyping data at baseline (*P* value < .05; *t* test; n = 13). Cluster frequencies of significant $CD4^+$ cluster 4 (CD4_C4) and $CD8^+$ cluster 1 (CD8_C1) are shown (as % of parent) on logit-scaled axes; the mean is indicated by the line. Cluster composition based on manually gated immune cell subsets is shown within the plot as a colored stacked bar chart. (B) PB blast reduction–associated immunophenotype clusters identified in PB after UMAP dimensionality reduction and FlowSOM clustering of high-dimensional cellular immunophenotyping data at baseline (*P* value < .05; *t* test; n = 43). Cluster frequencies of significant $CD8^+$ clusters 16, 6, and 1 (CD8_C16, CD8_C6, CD8_C1) are shown (as % of parent) on logit-scaled axes; the mean is indicated by the line. Cluster composition based on manually gated immune cell subsets is shown within the plot as a colored stacked bar chart. (C) Significantly expressed immune cell markers in each significant cluster from BM (panel A) and PB (panel B). The median marker intensity was tested for the respective cluster vs all other clusters (adjusted *P* value < .05; Wilcoxon rank sum test) and arrows indicate significant higher ↑ or lower ↓ intensity. Markers are ranked by significance; exhaustion markers are indicated in bold. (D) Baseline CD8 T-cell states in BM measured by scRNA-seq of BMMC samples (n = 14). Enrichment scores were calculated per cell and averaged per sample using previously described gene sets.[29] (E) WT1 messenger RNA target expression in PB shown as (normalized copy number) NCN measured by quantitative reverse transcription polymerase chain reaction; the line indicates the median (n = 30). Samples with WT1 below the level of quantification (BLQ) are shown in red. The dashed line indicates the value above which WT1 is considered to be overexpressed in normal PB (NCN = 50).[30] (F) Intracellular WT1 and cell surface HLA-A2 protein expression measured by flow cytometry in PB (left, n = 40) and BM (right, n = 27). Levels are shown as frequency (%) of blasts in PB or BM; the mean is indicated by the line and *P* values were determined after FDR adjustment (*t* test on logit-transformed values). (G) On-treatment dynamics of WT1+ (left) and HLA-A2+ (right) percentage of AML cells in BM measured by scRNA-seq of BMMC samples (n = 10). WT1+ / HLA-A+ cells defined by unique molecular identifier (UMI) >0; the color code indicates the clinical response at the time of sampling. (H) Distribution of %WT1+ cells within different AML subpopulations in BM at baseline as evaluated by scRNA-seq of BMMC samples (n = 14). WT1+ cells were defined by a UMI >0. (I) Change in AML subpopulations in BM at the time of progression as evaluated by scRNA-seq of BMMC samples (n = 9). Expansion defined as >5% increase relative to baseline; shrinkage defined as >5% decrease relative to baseline. (J) Percentage of WT1+/PSMB9+, WT1+/PSMB9–, and WT1– cells in expanding mono-like AML subpopulation at screening and the time point of disease progression as evaluated by scRNA-seq of BMMC samples (n = 9). WT1+ / PSMB9+ cells defined by a unique molecular identifier (UMI) >0. AML, acute myeloid leukemia; BMMC, bone marrow mononuclear cells; C, cluster; cDC, conventional dendritic cell; CM, central memory; CR, complete remission; CxDx, Cycle x Day x; EM, effector memory; FDR, false discovery rate; GMP, granulocyte-monocyte progenitors; hem., hematologic; LSPC, leukemia stem and progenitor cells; Mono, monocyte; NCN, normalized copy number; ProMono, pro-monocyte; PD, progressive disease; PSMB9, Proteasome 20S Subunit Beta 9; SCRN, screening; scRNA-seq, single-cell RNA sequencing; SD, stable disease; TEMRA, terminally differentiated effector memory cells re-expressing CD45RA; UMAP, Uniform Manifold Approximation and Projection; WT1, Wilms Tumor Protein 1.

analyses; J.A., T.B., M.Sun., and H.Y. analyzed data; and all authors had access to the primary clinical trial data and contributed to data interpretation and the writing and final approval of the manuscript.

Conflict-of-interest disclosure: M.H. reports receiving research support for the institution from AbbVie, AstraZeneca, Bristol Myers Squibb (BMS)/Celgene, Genentech, Genmab, Incyte, Johnson & Johnson, Merck, Novartis, Roche, and Takeda; and receiving personal honoraria from AbbVie, AstraZeneca, Genmab, Johnson & Johnson, Merck, Roche, and Takeda. K.K. reports being an employee of and owning shares in F. Hoffmann-La Roche. P.M. reports receiving research support from AbbVie, Astellas, BMS, Daiichi Sankyo, Janssen, Novartis, Pfizer, and Teva; serving a consultancy role for Astellas, BMS, Daiichi Sankyo, and Glycomimetics; participating in speakers' bureaus for AbbVie, Astellas, BMS, Daiichi Sankyo, Incyte, Janssen, Novartis, Pfizer, Sanofi, Servier, and Teva; and serving on advisory boards for AbbVie, Astellas, BMS, Daiichi Sankyo, Incyte, Janssen, Novartis, Pfizer, Sanofi, Servier, Syndax, and Teva. A.S. reports serving on advisory boards for Bayer, BMS, Eisai, Gilead, Merck Sharp & Dohme (MSD), Pfizer, and Servier; serving in a consultancy role for Incyte and Sanofi; and participating in speakers' bureaus for AbbVie, Amgen, ArQule, AstraZeneca, Bayer, BeiGene, BMS/Celgene, Eisai, Gilead, Eli Lilly, MSD, Novartis, Pfizer, Roche, Sandoz, Servier, and Takeda. H.-A.H reports receiving a honorarium, travel support, and consultancy fees from Roche. S. Vives reports receiving travel support, accommodation, and expenses from AbbVie, Astellas, Jazz Pharmaceuticals, Pfizer, and Servier; receiving research funding from Astellas; and serving as a consultant or in an advisory role (without honoraria) for AbbVie, Astellas, Jazz Pharmaceuticals, Pfizer, and Servier. T.-Y.C. reports serving in a consultancy role for AbbVie, Amgen, BMS/Celgene, Janssen, and Sanofi. S. Garciaz reports serving in a consultancy or advisory role for AbbVie, Astellas, BMS/Celgene, Jazz Pharmaceuticals, and Servier; and receiving travel grants from Gilead. O.S.G. reports receiving honoraria from AbbVie, BMS, and Jazz Pharmaceuticals; serving in a consultancy role for AbbVie, BMS, and Astellas; serving on advisory boards for BMS and Novartis; and receiving travel support from Jazz Pharmaceuticals and Servier. S.-P.Y. received advisory board and/or lecture fees from AbbVie, Amgen, Astellas, Astex Pharmaceuticals, AstraZeneca, BeiGene, BMS, Janssen Pharmaceuticals, Novartis, Sanofi, and Takeda. K.Y. reports serving in a consultancy role for BMS/Celgene, F. Hoffmann-La Roche, GlaxoSmithKline (GSK), Jazz Pharmaceuticals, Novartis, Pfizer, Shattuck Labs, Taiho Oncology, and Takeda; receiving research funding from Astex Pharmaceuticals, F. Hoffmann-La Roche/Genentech, Forma Therapeutics, Geron Corporation, Gilead Sciences, Janssen, Jazz Pharmaceuticals, Novartis, and Treadwell Therapeutics; and receiving honoraria from AbbVie, Novartis, and Taiho. J.E. reports receiving research support from AbbVie, Jazz Pharmaceuticals, and Novartis; and providing scientific advice to AbbVie, Amgen, Astellas, BMS, Jazz Pharmaceuticals, Novartis, and Pfizer. A.B. reports receiving honoraria from AbbVie, Amgen, Astellas, Novartis, Pfizer, and Takeda; serving in an advisory role for Senti Bio and Shoreline; and participating in speakers' bureaus for Amgen and BMS. S.F. reports serving in a consultancy role for Gilead; receiving research funding from Amgen; receiving honoraria from Amgen, BMS, Gilead, Novartis, Pfizer, and Servier; participating in speakers' bureaus for Amgen, BMS, Gilead, Novartis, Pfizer, and Servier; and serving on the board of directors or advisory committees for Amgen, BMS, Gilead, Novartis, Pfizer, and Servier. A.C.B. reports being an employee of Roche Diagnostic GmbH and owning shares in F. Hoffmann-La Roche. J.A. reports being an employee of and owning shares in F. Hoffmann-La Roche and biotechnology funds, which may indirectly include pharmaceutical company shares. M. Sun, Y.M.M., G.S., H.Y., H.H., T.B., S.S., and S.N. report being employees of and owning shares in F. Hoffmann-La Roche. T.R. and S. Vauleon report being employees of F. Hoffmann-La Roche. C.K. reports being an employee of F. Hoffmann-La Roche at the time of the study and owning shares in F. Hoffmann-La Roche; and receiving patents/royalties from F. Hoffmann-La Roche. M.R. reports being an employee of F. Hoffmann-La Roche at the time of the study and owning shares in F. Hoffmann-La Roche. N.K. reports being an employee of and owning shares in F. Hoffmann-La Roche; and reports owning shares in Jazz Pharmaceuticals. M. Subklewe reports receiving research support from Amgen, BMS/Celgene, Gilead/Kite, Janssen, Miltenyi Biotec, Molecular Partners, Novartis, Roche, Seagen, Takeda; participating in speakers' bureaus for AstraZeneca, BMS, Gilead/Kite, GSK, Janssen, Novartis, Pfizer, Roche, Springer Healthcare; serving in a consultancy role or on an advisory board for AbbVie, Amgen, Autolus, AvenCell, BMS, CanCell Therapeutics, Genmab US, Gilead, Ichnos Sciences, Incyte Biosciences, Interius BioTherapeutics, Janssen, Miltenyi Biomedicine, Molecular Partners, Nektar Therapeutics, Novartis, Orbital Therapeutics, Pfizer, Roche, Sanofi, Scare, Takeda; and receiving travel support from Gilead, Pfizer, and Roche. The remaining authors declare no competing financial interests.

ORCID profiles: M.H., 0000-0003-3873-1741; P.M., 0000-0002-3275-5593; A.S., 0000-0003-1709-9492; T.-Y.C., 0000-0001-7099-8054; K.Y., 0000-0002-2572-9952; A.C.B., 0000-0001-9302-3786; J.A., 0000-0002-2159-2880; C.K., 0000-0001-7594-7280; G.S., 0000-0003-4889-8596; M.R., 0000-0003-0295-7730; M.S., 0000-0001-9154-9469.

Correspondence: Marion Subklewe, Department of Medicine III, University Hospital, Ludwig Maximilian University Munich, Marchioninistrasse 15, 81377 Munich, Germany; email: marion.subklewe@med.uni-muenchen.de; and Nino Keshelava, Roche Pharma Research and Early Development, Oncology, Roche Innovation Center Zurich, Wagistrasse 10, 8952 Schlieren, Switzerland; email: nino.keshelava@roche.com.

References

1. Döhner H, Wei AH, Appelbaum F, et al. Diagnosis and management of AML in adults: 2022 recommendations from an international expert panel on behalf of the ELN. *Blood*. 2022;140(12):1345-1377.

2. Stubbins R, Francis A, Kuchenbauer F, Sanford D. Management of acute myeloid leukemia: a review for general practitioners in oncology. *Curr Oncol*. 2022;29(9):6245-6259.

3. National Cancer Institute Surveillance, Epidemiology, and End Results Program. Cancer stat facts: leukemia - acute myeloid leukemia (AML). Accessed 28 May 2025. https://seer.cancer.gov/statfacts/html/amyl.html
4. Percival M-E, Estey E. Emerging treatments in acute myeloid leukemia: current standards and unmet challenges. *Clin Adv Hematol Oncol*. 2017;15(8):632-642.
5. Morris V, Ghazi H, Fletcher D, Guinn B. A direct comparison, and prioritisation, of the immunotherapeutic targets expressed by adult and paediatric acute myeloid leukaemia cells: a systematic review and meta-analysis. *Int J Mol Sci*. 2023;24(11):9667.
6. Augsberger C, Hänel G, Xu W, et al. Targeting intracellular WT1 in AML with a novel RMF-peptide-MHC-specific T-cell bispecific antibody. *Blood*. 2021;138(25):2655-2669.
7. Xu G, Luo Y, Wang H, Wang Y, Liu B, Wei J. Therapeutic bispecific antibodies against intracellular tumor antigens. *Cancer Lett*. 2022;538:215699.
8. Ariyaratana S, Loeb D. The role of the Wilms tumour gene (WT1) in normal and malignant haematopoiesis. *Expert Rev Mol Med*. 2007;9(14):1-17.
9. Ahmed S, Elsherif M, Yassin D, et al. Integration of measurable residual disease by WT1 gene expression and flow cytometry identifies pediatric patients with high risk of relapse in acute myeloid leukemia. *Front Oncol*. 2024;14:1340909.
10. Gianfaldoni G, Mannelli F, Ponziani V, et al. Early reduction of WT1 transcripts during induction chemotherapy predicts for longer disease free and overall survival in acute myeloid leukemia. *Haematologica*. 2010;95(5):833-836.
11. Arai S, Tachibana T, Izumi A, et al. WT1-guided pre-emptive therapy after allogeneic hematopoietic stem cell transplantation in patients with acute myeloid leukemia. *Int J Hematol*. 2024;120(3):337-346.
12. Chau Y-Y, Brownstein D, Mjoseng H, et al. Acute multiple organ failure in adult mice deleted for the developmental regulator Wt1. *PLoS Genet*. 2011;7(12):e1002404.
13. Chapuis A, Egan D, Bar M, et al. T cell receptor gene therapy targeting WT1 prevents acute myeloid leukemia relapse post-transplant. *Nat Med*. 2019;25(7):1064-1072.
14. Anguille S, van de Velde A, Smits E, et al. Dendritic cell vaccination as postremission treatment to prevent or delay relapse in acute myeloid leukemia. *Blood*. 2017;130(15):1713-1721.
15. Lichtenegger FS, Schnorfeil FM, Rothe M, et al. Toll-like receptor 7/8-matured RNA-transduced dendritic cells as post-remission therapy in acute myeloid leukaemia: results of a phase I trial. *Clin Transl Immunology*. 2020;9(3):e1117.
16. Döhner H, Estey E, Grimwade D, et al. Diagnosis and management of AML in adults: 2017 ELN recommendations from an international expert panel. *Blood*. 2017;129(4):424-447.
17. Heuser M, Freeman S, Ossenkoppele G, et al. 2021 update on MRD in acute myeloid leukemia: a consensus document from the European LeukemiaNet MRD Working Party. *Blood*. 2021;138(26):2753-2767.
18. Proctor WR, Foster AJ, Vogt J, et al. Utility of spherical human liver microtissues for prediction of clinical drug-induced liver injury. *Arch Toxicol*. 2017;91(8):2849-2863.
19. van de Donk N, Zweegman S. T-cell-engaging bispecific antibodies in cancer. *Lancet*. 2023;402(10396):142-158.
20. Ball K, Dovedi S, Vajjah P, Phipps A. Strategies for clinical dose optimization of T cell-engaging therapies in oncology. *MAbs*. 2023;15(1):2181016.
21. Liu S, Yin G, Yuan Y. Bayesian data augmentation dose finding with continual reassessment method and delayed toxicity. *Ann Appl Stat*. 2013;7(4):1837-2457.
22. Zhu J, Sabanés Bové D, Liao Z, Beyer U, Yung G, Sarkar S. Rolling continual reassessment method with overdose control: an efficient and safe dose escalation design. *Contemp Clin Trials*. 2021;107:106436.
23. Leclercq G, Haegel H, Schneider A, et al. Src/lck inhibitor dasatinib reversibly switches off cytokine release and T cell cytotoxicity following stimulation with T cell bispecific antibodies. *J Immunother Cancer*. 2021;9(7):e002582.
24. Bröske AME, Korfi K, Belousov A, et al. Pharmacodynamics and molecular correlates of response to glofitamab in relapsed/refractory non-Hodgkin lymphoma. *Blood Adv*. 2022;6(3):1025-1037.
25. Uy G, Aldoss I, Foster M, et al. Flotetuzumab as salvage immunotherapy for refractory acute myeloid leukemia. *Blood*. 2021;137(6):751-762.
26. Ravandi F, Walter R, Subklewe M, et al. Updated results from phase I dose-escalation study of AMG 330, a bispecific T-cell engager molecule, in patients with relapsed/refractory acute myeloid leukemia (R/R AML). *J Clin Oncol*. 2020;38(suppl 15):7508.
27. Ravandi F, Bashey A, Foran J, et al. Phase 1 study of vibecotamab identifies an optimized dose for treatment of relapsed/refractory acute myeloid leukemia. *Blood Adv*. 2023;7(21):6492-6505.
28. Subklewe M, Stein A, Walter R, et al. Preliminary results from a Phase 1 first-in-human study of AMG 673, a novel half-life extended (HLE) anti-CD33/CD3 BiTE® (Bispecific T-Cell Engager) in patients with relapsed/refractory (R/R) acute myeloid leukemia (AML). *Blood*. 2019;134(suppl 1):833.
29. van der Leun A, Thommen D, Schumacher T. CD8+ T cell states in human cancer: insights from single-cell analysis. *Nat Rev Cancer*. 2020;20(4):218-232.
30. Cilloni D, Renneville A, Hermitte F, et al. Real-time quantitative polymerase chain reaction detection of minimal residual disease by standardized WT1 assay to enhance risk stratification in acute myeloid leukemia: a European LeukemiaNet study. *J Clin Oncol*. 2009;27(31):5195-5201.
31. Joller N, Lozano E, Burkett P, et al. Treg cells expressing the coinhibitory molecule TIGIT selectively inhibit proinflammatory Th1 and Th17 cell responses. *Immunity*. 2014;40(4):569-581.

32. Kurtulus S, Sakuishi K, Ngiow S-F, et al. TIGIT predominantly regulates the immune response via regulatory T cells. *J Clin Invest*. 2015;125(11):4053-4062.
33. Lahman MC, Schmitt TM, Paulson KG, et al. Targeting an alternate Wilms' tumor Antigen-1 peptide bypasses immunoproteasome dependency. *Sci Trans Med*. 2022;14(631):eabg8070.
34. Kantarjian H, DiNardo C, Nogueras-Gonzalez G, et al. Results of second salvage therapy in 673 adults with acute myelogenous leukemia treated at a single institution since 2000. *Cancer*. 2018;124(12):2534-2540.
35. Allen C, Zeidan A, Bewersdorf JP. BiTEs, DARTS, BiKEs and TriKEs - are antibody based therapies changing the future treatment of AML? *Life*. 2021;11(6):465.
36. Lamble A, Lind E. Targeting the immune microenvironment in acute myeloid leukemia: a focus on T cells immunity. *Front Oncol*. 2018;8:213.
37. Shimabukuro-Vornhagen A, Gödel P, Subklewe M, et al. Cytokine release syndrome. *J Immunother Cancer*. 2018;6(1):56.
38. Chinnici A, Beneforti L, Pegoraro F, et al. Approaching hemophagocytic lymphohistiocytosis [published correction appears in Front Immunol. 2024:15:1369687]. *Front Immunol*. 2023;14:1210041.
39. Löfstedt A, Jädersten M, Meeths M, Henter J-I. Malignancy-associated hemophagocytic lymphohistiocytosis in Sweden: incidence, clinical characteristics, and survival. *Blood*. 2024;143(3):233-242.
40. Teachey D, Rheingold S, Maude S, et al. Cytokine release syndrome after blinatumomab treatment related to abnormal macrophage activation and ameliorated with cytokine-directed therapy. *Blood*. 2013;121(26):5154-5157.
41. Schram AM, Berliner N. How I treat hemophagocytic lymphohistiocytosis in the adult patient. *Blood*. 2015;125(19):2908-2914.
42. Strenger V, Merth G, Lackner H, et al. Malignancy and chemotherapy induced haemophagocytic lymphohistiocytosis in children and adolescents–a single centre experience of 20 years. *Ann Haemat*. 2018;97(6):989-998.
43. Bauchmuller K, Manson JJ, Tattersall R, et al. Haemophagocytic lymphohistiocytosis in adult critical care. *J Intensive Care Soc*. 2020;21(3):256-268.
44. Delavigne K, Bérard E, Bertoli S, et al. Hemophagocytic syndrome in patients with acute myeloid leukemia undergoing intensive chemotherapy. *Haematologica*. 2014;99(3):474-480.
45. Narayan R, Piérola AA, Donnellan WB, et al. First- in- human study of JNJ- 67571244, a CD33 × CD3 bispecific antibody, in relapsed/refractory acute myeloid leukemia and myelodysplastic syndrome. *Clin Transl Sci*. 2024;17(3):e13742.
46. Cortes-Selva D, Perova T, Skerget S, et al. Correlation of immune fitness with response to teclistamab in relapsed/refractory multiple myeloma in MajesTEC-1. *Blood*. 2024;144(6):615-628.
47. Nassiri S, Schmeing S, Leclercq G, et al. Molecular mechanisms underlying response and resistance to glofitamab. *Blood*. 2023;142(suppl 1):1619-1620.
48. Knaus H, Berglund S, Hackl H, et al. Signatures of CD8+ T cell dysfunction in AML patients and their reversibility with response to chemotherapy. *JCI Insight*. 2018;3(21):e120974.
49. Yan Y, Upadhyaya R, Zhang VW, Berg T. Epigenetic maintenance strategies after allogeneic stem cell transplantation in acute myeloid leukemia. *Exp Hematol*. 2022;109:1-10.e1.
50. Hänel G, Schönle A, Neumann AS, et al. Combining venetoclax and azacytidine with T-cell bispecific antibodies for treatment of acute myeloid leukemia: a preclinical assessment. *Leukemia*. 2024;38(2):398-402.
51. Atilla PA, McKenna MK, Watanabe N, Mamonkin M, Brenner MK, Atilla E. Combinatorial antigen targeting strategies for acute leukemia: application in myeloid malignancy. *Cytotherapy*. 2022;24(3):282-290.
52. Ma H, Padmanabhan IS, Parmar S, Gong Y. Targeting CLL-1 for acute myeloid leukemia therapy. *J Hematol Oncol*. 2019;12(1):41.
53. Yang J, Chen M, Ye J, Ma H. Targeting PRAME for acute myeloid leukemia therapy. *Front Immunol*. 2024;15:1378277.
54. Stroopinsky D, Rosenblatt J, Ito K, et al. MUC1 is a potential target for the treatment of acute myeloid leukemia stem cells. *Cancer Res*. 2013;73(17):5569-5579.
55. Zhu S, Zhang T, Zheng L, et al. Combination strategies to maximize the benefits of cancer immunotherapy. *J Hematol Oncol*. 2021;14(1):156.
56. Kallingal A, Olszewski M, Maciejewska N, Brankiewicz W, Baginski M. Cancer immune escape: the role of antigen presentation machinery. *J Cancer Res Clin Oncol*. 2023;149(10):8131-8141.
57. Meraviglia-Crivelli D, Zheleva A, Barainka M, Moreno B, Villanueva H, Pastor F. Therapeutic strategies to enhance tumor antigenicity: making the tumor detectable by the immune system. *Biomedicines*. 2022;10(8):1842.